Progress in Oceanography 112–113 (2013) 49–59

Contents lists available at SciVerse ScienceDirect

Progress in Oceanography

journal homepage: www.elsevier.com/locate/pocean

The role of *Synechococcus* in vertical flux in the Costa Rica upwelling dome

Michael R. Stukel [a,*], Moira Décima [a], Karen E. Selph [b], Darcy A.A. Taniguchi [a], Michael R. Landry [a]

[a] Scripps Institution of Oceanography, University of California at San Diego, La Jolla, CA, United States
[b] Department of Oceanography, University of Hawaii at Manoa, Honolulu, HI 96822, United States

ARTICLE INFO

Article history:
Received 24 October 2012
Received in revised form 21 April 2013
Accepted 23 April 2013
Available online 4 May 2013

ABSTRACT

Despite evidence that picophytoplankton contribute to export from marine pelagic ecosystems to some extent, few field studies have experimentally evaluated the quantitative importance of that flux or specifically assessed the relative strengths of alternate ecological pathways in transporting picophytoplankton carbon to depth. In experimental studies in the Costa Rica Dome (CRD), we used a combination of methods – flow cytometry (FCM), microscopy, pigments, dilution assays, mesozooplanton gut contents and sediment traps – to follow production, grazing and export fates of the dominant picophytoplankter, *Synechococcus* spp. (*Syn*), relative to the total phytoplankton community. *Syn* accounted for an average of 25% (range 9–50%) of total phytoplankton production during four 4-day drifter experiments at CRD sites. During the same experiments, sediment trap deployments at the base of the euphotic zone measured total organic carbon export ranging from 50 to 72 mg C m^{-2} d^{-1}. Flow cytometry measurements of the trap samples showed that only 0.11% of this carbon was recognizable as ungrazed sinking *Syn*. Phycoerythrin (PE) measurements on the same samples, which we attributed mostly to transport of intact cells in mesozooplankton fecal pellets, gave export contributions of unassimilated *Syn* eight-times higher than ungrazed sinking cells, though still <1% of total carbon. Grazing of mesozooplankton on *Syn* was confirmed by PE measurements of mesozooplankton guts and the visual presence of *Syn* cells in fecal pellets. Microzooplankton grazing estimates from dilution experiments, combined with degradation rates of mesozooplankton fecal material in the water column, allowed us to estimate indirectly the additional flux of carbon transferred through protozoan grazers before being exported as mesozooplankton fecal pellets. Assuming one to three protozoan trophic steps, this *Syn* pathway contributed on average an additional 0.5–5.7% of organic carbon flux. A similar budget for total phytoplankton, based on chlorophyll *a* and phaeopigments was consistent with fecal pellets as the dominant mechanism of sinking carbon. Therefore, while *Syn* sinking as ungrazed cells or aggregates were minor components of export, the indirect trophic pathway involving mesozooplankton predation on protozoan consumers of *Syn* comprised the major mode of bulk carbon export for *Syn*-generated primary production.

1. Introduction

Phototrophic cells in the picoplankton size class (<2 μm) are known to be major contributors to phytoplankton biomass and production in the open ocean (Li et al., 1983; Brown et al., 1999; Poulton et al., 2006). Their role in vertical carbon flux, however, is both poorly quantified and heavily debated. Generally, it is believed that picophytoplankton are too small to sink individually or to be grazed efficiently by most fecal pellet-producing mesozooplankton, making them less likely to contribute significantly to carbon export compared to larger taxa (Michaels and Silver, 1988). Inverse modeling studies initially questioned this interpretation, inferring the need for large fluxes of ungrazed picophytoplankton to balance their estimates of system-level rates (e.g. Richardson and Jackson, 2007). Although that inference has itself been criticized (Stukel and Landry, 2010), such models were important in highlighting the potential importance of aggregation mechanisms to enhance gravitational sinking of the ungrazed picophytoplankton production. Among direct observations, distinguishable picophytoplankton cells are often present in flow cytometric and microscopic examinations of sediment trap contents, though at concentrations that account for only a small fraction of total carbon flux (Silver and Gowing, 1991; Rodier and Le Borgne, 1997; Waite et al., 2000). Diagnostic pigments that might be indicative of much larger concentrations of partially degraded picophytoplankton have also been detected in sediment trap material (Lamborg et al., 2008) and mesopelagic regions of the water column (Lomas and Moran, 2011). In addition, genetic sequencing, at least at one

Abbreviations: CRD, Costa Rica Dome; ETP, eastern tropical Pacific; FCM, flow cytometry; PE, phycoerythrin; Phaeo, phaeopigments; *Syn*, *Synechococcus*; CE, conversion efficiency; EE, egestion efficiency; GGE, gross growth efficiency.

* Corresponding author. Present address: Horn Point Laboratory, University of Maryland Center for Environmental Science, Cambridge, MD 21613, United States. Tel.: +1 (815)258 3875.
E-mail address: mstukel@hpl.umces.edu (M.R. Stukel).

0079-6611/$ - see front matter © 2013 Elsevier Ltd. All rights reserved.
http://dx.doi.org/10.1016/j.pocean.2013.04.003

site, has shown picoeukaryotes to be overrepresented in sediment trap material relative to diatoms when compared to the overlying water column (Amacher et al., 2009).

Despite mounting evidence that picophytoplankton contribute to export to some extent, few field studies have experimentally evaluated the quantitative importance of that flux, and, perhaps more importantly, none have specifically assessed the relative strengths of alternate ecological pathways in transporting picophytoplankton carbon to depth. Three distinct pathways exist for concentrating and facilitating the export of picophytoplankton carbon, each with its own efficiency of transport and implication for plankton ecology. Picophytoplankton may be incorporated into sinking aggregates (Waite et al., 2000; Richardson and Jackson, 2007). They may be grazed by mesozooplankton, either individually (Pfannkuche and Lochte, 1993; Gorsky et al., 1999) or as a by-product of feeding on aggregates (Wilson and Steinberg, 2010), and exported as unassimilated material within fecal pellets (Pfannkuche and Lochte, 1993; Waite et al., 2000). They may also be grazed by protozoans in the microbial portion of the food web, with these in turn being consumed and incorporated into fecal pellets by mesozooplankton. This latter mechanism constitutes an indirect transport pathway of picophytoplankton carbon to depth (Stukel and Landry, 2010) that may retain little or no indication (pigments or DNA) of its origins as picophytoplankton production.

The Costa Rica Dome (CRD) is a unique region of open-ocean upwelling and shoaling of isopycnals in the eastern tropical Pacific (ETP), centered at 9°N, 90°W (Fiedler, 2002). One property of the region is its remarkably large populations of the picocyanobacteria, *Synechococcus* spp. (*Syn*), with concentrations typically exceeding 10^5 cells mL^{-1} and often $>10^6$ cells mL^{-1} (Li et al., 1983; Saito et al., 2005). The CRD thus offers a unique opportunity to study the export flux role of a dominant picophytoplankton that is readily distinguished and quantified by microscopy, flow cytometry and characteristic pigments. Here we measure phytoplankton (total and *Syn*) standing stocks and growth rates, grazing by micro- and mesozooplankton, and vertical fluxes in four water parcels across the CRD. Based on analyses of *Syn* by flow cytometry and the diagnostic pigment phycoerythrin (PE), and in comparison to a pigment-carbon budget for total phytoplankton, we show (1) that *Syn* sinking as ungrazed cells or aggregates is a minor component of export, (2) that mesozooplankton grazing/fecal pellet transport provides the main export mechanism for distinguishable *Syn* cells from the euphotic zone, and (3) that the indirect trophic pathway of mesozooplankton predation on protozoan primary consumers of *Syn* comprises the major mode of bulk carbon export for *Syn*-generated primary production.

2. Methods

2.1. Experimental design and sampling

Using a semi-Lagrangian experimental design similar to that in Landry et al. (2009), we conducted four experimental studies involving water-column sampling and rate measurements of phytoplankton production and growth, grazing losses to micro- and mesozooplankton, and export fluxes into sediment traps. These were done on the CRD FLUZiE (Flux and Zinc Experiments) cruise aboard R/V Melville in July 2010. For each 4-day study, which we called an experimental "cycle", we followed a marked water parcel with a satellite-tracked drift array with a holey-sock drogue (3×1-m) centered at 15-m depth. The drifter served both as the moving frame of reference for our sampling and experimental measurements and as an in situ incubator for daily bottle experiments for rate determinations that were attached in coarse net bags to a tether line beneath the surface float. We also deployed for the duration of each 4-day cycle a second drogued drift array with sediment traps at two depths to quantify particulate fluxes from the euphotic zone. Seawater samples were collected from Niskin bottles mounted on a CTD-equipped rosette, typically within 100 m of the drift array. Early morning samples (0200 local time) from the Niskin bottles were used both for daily assessments of standing stocks and to set up dilution experiments. Oblique net tows through the full euphotic zone were taken to measure mesozooplankton biomass and gut pigment contents.

We used a combination of flow cytometry (FCM), microscopy and pigment analyses to follow the production and fate of *Syn* and the total phytoplankton community through various processes (Table 1). Production and microzooplankton (protozoan) grazing rates were determined from daily dilution incubations at 8 depths in the euphotic zone. Grazing by mesozooplankton was assessed from gut content analyses of PE and phaeopigments and followed to its fate as unassimilated *Syn* and total phytoplankton in fecal pellets collected in the sediment traps. Finally, we used protozoan grazing measurements, pigment degradation rates, and gross growth efficiency assumptions to constrain estimates of the amount of *Syn* and total phytoplankton transported to depth in fecal pellets by indirect trophic transfer.

2.2. Phytoplankton biomass assessments

We used various FCM, pigment and microscopy methods to estimate water-column standing stocks and cell:pigment or C:pigment ratios for both *Syn* and the total phytoplankton community. Stock estimates for *Syn* came from direct FCM cell counts, assuming a cell carbon content of 101 fg C $cell^{-1}$ (Garrison et al., 2000), and from measurements of the cyanobacteria marker pigment phycoerythrin (PE). For total phytoplankton, we used Chl *a* as the pigment indicator and combined FCM (photosynthetic bacteria) and epifluorescence microscopy (eukaryotes) to assess total carbon biomass.

FCM analyses were done with live samples onboard ship and with frozen preserved samples in the laboratory. Different instruments were used but with very similar results for *Synechococcus* (lab cells $mL^{-1} = -1771 + 0.974 * \text{ship cells } mL^{-1}$; $r = 0.99$, $n = 160$ paired samples taken from the same Niskin bottles). Results from the ship instrument (a Beckman-Coulter XL with a 15-mW 488-nm argon ion laser) are used in the present study for all water-column stock and rate assessments for *Syn* and for sediment trap

Table 1
Assessment of export pathways. Carbon export (stemming from either *Syn* or total phytoplankton) was determined for three distinct pathways: Sinking of ungrazed cells and aggregates, sinking of unassimilated cells within mesozooplankton fecal pellets, and trophic transfer through protozoans to mesozooplankton. PrGr is protozoan grazing, GGE is protozoan gross growth efficiency, TL is the number of protozoan trophic levels separating *Syn* from mesozooplankton, PigDeg is the pigment degradation rate prior to export (includes degradation within mesozooplankton guts and remineralization of fecal pellets in the euphotic zone and is calculated as the ratio of sediment trap pigment flux to mesozooplankton pigment ingestion).

Pathway	Sinking cells/aggregates	Herbiv. fecal pellets	Trophic transfer
Assessment	Direct	Direct	Indirect
Measurements	Flow cytometry	Pigments	Protozoan grazing, pigment degradation
Calculation	*Syn* flux × Carbon:*Syn*	PE flux × Carbon:PE	$PrGr \times GGE^{TL} \times PigDeg$

analyses (below). Results from the lab cytometer (Beckman-Coulter Altra with 200-mW UV and 1-W 488-nm argon ion lasers) are used only for total phytoplankton carbon biomass estimates because that instrument gave more reliable counts for *Prochlorococcus*. For the shipboard cytometer, an Orion syringe pump delivered 2.2-mL samples at a rate of 0.44 mL min^{-1} (Selph et al., 2001). *Syn* were distinguished from light scatter (forward and 90° side scatter), chlorophyll and PE fluorescence, normalized to 6-μm fluorescent calibration beads. For the lab analyses, 2-mL samples were preserved (0.5% paraformaldehyde, final concentration), flash frozen in liquid nitrogen, and later stained with Hoechst 33342 at 1 μg mL^{-1} final concentration before analysis (Monger and Landry, 1993). Fluorescence signals were normalized to 0.5 and 1.0-μm yellow-green (YG) polystyrene beads (Polysciences Inc., Warrington, PA). Listmode data files (FCS 2.0 format) of cell fluorescence and light-scatter properties were acquired with Expo32 software (Beckman-Coulter) and used with FlowJo software (Tree Star, Inc., www.flowjo.com). For biomass estimates, we used carbon contents of 32 and 101 fg C $cell^{-1}$ for *Prochlorococcus* and *Synechococcus*, respectively (Garrison et al., 2000).

Samples (250 mL) taken for fluorometric analyses of Chl *a* were immediately filtered onto GF/F filters, and the Chl *a* extracted with 90% acetone in a dark freezer for 24 h. Extracted samples were shaken, warmed in the dark to room temperature, settled and quantified on a calibrated Turner Designs model 10 fluorometer (Strickland and Parsons, 1972). PE was measured using the glycerol uncoupling method of Wyman (1992). Water-column samples were vacuum-filtered sequentially through a 20-μm filter to remove larger particles and a 0.6-μm polycarbonate filter to retain small cyanobacteria. The filters were then transferred to 20-mL glass scintillation vials with a saline 50% glycerol solution (35 g L^{-1} NaCl, final concentration), briefly shaken on a vortex mixer, and refrigerated for 2–24 h to allow the cells to become suspended in solution. Fluorescence was measured on a Turner Designs TD-700 Fluorometer with a PE filter set (excitation 544 nm, emission 577 nm). The fluorometer was calibrated with a commercial R-phycoerythrin standard (Wyman, 1992; Dore et al., 2002).

Epifluorescence microscopy was done for a subset of sampling depths ($n = 120$) sufficient to determine the mean C:Chl *a* ratio for the phytoplankton assemblage. Details of the methods are the same as Taylor et al. (2012). Seawater samples (500 mL) were preserved and cleared according to a modified protocol from Sherr and Sherr (1993), with sequential additions of 260 μL of alkaline Lugol's solution, 10 mL of buffered Formalin and 500 μL of sodium thiosulfate, followed by staining with 1 mL of proflavin (0.33% w/v) and 1 mL of DAPI (0.01 mg mL^{-1}). Aliquots of 50 mL were filtered onto 25-mm, 0.8-μm pore-size black polycarbonate filters to determine concentrations of nanophytoplankton, and the remaining 450-mL samples were filtered onto black 8.0-μm polycarbonate filters to determine concentrations of larger cells (microplankton). Filters were mounted onto glass slides and digitally imaged in Z-stack mode at 630X (nanoplankton) and 200X (microplankton) using an automated Zeiss Axiovert 200 M inverted compound microscope. A minimum of 20 random positions were imaged for each slide, with each Z-stack level and position consisting of four fluorescent channels: Chl *a*, DAPI, FITC and phycoerythrin. The separate images were combined to produce one composite best-in-focus 24-bit RGB image for each position, and these were processed and analyzed using ImagePro software. Phytoplankton biovolumes (BV; μm^3) were calculated from the length (L) and width (W) measurements of each cell using the geometric formula of a prolate sphere (BV = 0.524 LWH), where unmeasured height (H) was estimated as W for diatoms and 0.5 W for flagellates (Taylor et al., 2012). Biomass was calculated as carbon (C; pg $cell^{-1}$) using the equations of Menden-Deuer and Lessard (2000): $C = 0.288\ BV^{0.811}$ for diatoms and $C = 0.216\ BV^{0.939}$ for non-diatoms.

2.3. Dilution experiments

Rates of growth, production and protozoan grazing were estimated for *Syn* and for the total phytoplankton community from the results of 2-treatment dilution experiments (Landry et al., 1984, 2008) incubated in situ at 8 depths on the drift array, 4 times per cycle. Following the procedures described in Landry et al. (2009), we prepared one diluted treatment and one control bottle (2.7-L polycarbonate) per depth, respectively, with 33% whole seawater (diluted with 0.1-μm Suporcap filtered seawater) and 100% seawater collected from Niskin bottles from the CTD-rosette. Initial FCM samples were taken from each bottle prior to deployment, and initial samples for Chl *a* were taken from the same Niskin bottle as the incubation water. The experiments were incubated for 24 h (deployment/recovery ~0430 local time). Upon recovery, the incubation bottles were subsampled for FCM and Chl *a*. Instantaneous grazing rates (m) on Chl *a* or *Syn* cells were determined from net measured growth rates in treatment (k_t) and control bottles (k_c) as $m = (k_t - k_c)/(1–0.33)$. Instantaneous growth rates were determined as $\mu = k_c + m$. Biomass production (PP) and grazing (PG) estimates were computed as $PP = \mu * B_0$ and $PG = m * B_0$, where B_0 is the initial (and in situ) phytoplankton biomass. For these, we used carbon biomass conversions of 101 pg C $cell^{-1}$ for *Syn* and C:Chl = 73 for total phytoplankton (see results).

2.4. Mesozooplankton grazing

Mesozooplankton were sampled daily with paired day-night oblique tows to 150-m depth with a ring net (0.71 m^2, 202-μm mesh size), for a total of 4 paired measurements per experimental cycle. A General Oceanics flowmeter was attached across the net mouth to record volume filtered, and a Vyper Suunto dive computer was fastened to the net frame to record tow depth and duration. Immediately upon recovery, organisms were anesthetized with carbonated water (Kleppel and Pieper, 1984). The samples were then split with a Folsom splitter for biomass and gut pigment determinations. Typically, 1/8 sample splits were filtered onto 200-μm Nitex filters for gut pigment analyses for phaeopigments (Phaeo) and PE and flash frozen in liquid N_2. Phaeo samples were thawed and extracted with a tissue homogenizer in 90% acetone, and the homogenate was centrifuged for 5 min at 3000 rev min^{-1} to remove particulates. Concentrations of Phaeo were then measured using a Turner 10AU fluorometer (Strickland and Parsons, 1972). PE samples (only one pair of samples per cycle) were later washed from filters with glycerol saline solution, ground with a tissue homogenizer to release gut contents, and centrifuged to separate the supernatant from pellets containing crushed mesozooplankton carcasses. After refrigeration for 2–24 h, fluorescence was measured on a Turner Designs TD-700 fluorometer with a PE filter set.

For each analysis, we computed the depth-integrated concentration of gut pigment (Phaeo, PE) in the euphotic zone as:

$$\mathrm{GPC} = \frac{pig * f * D}{vol} \quad (1)$$

where GPC is gut pigment content (mg m^{-2}), *pig* is the measured pigment value (mg), f is fraction of sample analyzed, D is depth of tow (m) and *vol* is the volume of water filtered (m^3) (Décima et al., 2011). To compute grazing rates from gut content measurements, we utilized the gut turnover rate of 2.1 h^{-1} measured for zooplankton in the Equatorial Pacific (Zhang et al., 1995), where temperature conditions were similar to the CRD.

2.5. Sediment traps

We deployed VERTEX-style sediment traps (8:1 aspect ratio, 7-cm diameter, with a baffle of 14 smaller tubes tapered at the top) on a satellite-tracked drifter array at two depths (base of the euphotic zone and 150 m) at the beginning of each 4-day experimental cycle, and recovered them at the end. At each depth, 8–12 replicate tubes were held vertically in place on a PVC cross piece (Knauer et al., 1979). All tubes were filled before deployment with a slurry of 0.1-μm filtered seawater amended with 50 g L^{-1} NaCl and 1% final concentration formalin. Upon recovery, water above the density interface in each tube was gently removed by peristaltic pump, and the samples were filtered through a 200-μm Nitex filter. Filters were examined under a dissecting microscope to remove zooplankton swimmers, and the remaining material was rinsed off the filter and returned to the sample. We do not believe that substantial numbers of mesozooplankton passed through the 200-μm Nitex mesh, because a few exploratory net tows with a 100-μm mesh suggested that 100–200-μm sized organisms comprised an insignificant portion of the total mesozooplankton biomass and small mesozooplankton are typically weak vertical migrators.

For analyses, 1/8 to 1/4 of the tube contents was filtered onto a 0.6-μm filter for PE measurements and 1/4 of the contents was filtered onto a pre-combusted GF/F filter for measurement of particulate organic carbon (POC). Smaller subsamples (50 mL) of the well-mixed trap contents were also removed for Chl *a* and phaeopigment (Phaeo) determinations, for FCM enumeration of *Syn* cells (20 mL), and for epifluoresence microscopy (EPI) of larger intact cells (50 mL). Chl *a* and Phaeo concentrations were measured, as above, by the fluorometric acidification method. POC analyses were done with a Costech 4010 Elemental combustion analyzer, following acidification to remove inorganic carbon. PE samples were ground with a tissue homogenizer prior to addition of glycerol saline solution and refrigerated for 2–24 h. Fluorescence was measured on a Turner Designs TD-700 fluorometer with PE filter set.

FCM subsamples were stored on ice in the dark until analyzed within 1–6 h of collection with the shipboard cytometer (Beckman-Coulter XL). Just prior to analysis, the samples were briefly vortexed and pre-filtered through 200-μm Nitex mesh to disrupt delicate aggregates while keeping fecal pellets largely intact (fragile salp fecal pellets were rare in the sediment trap samples). *Syn* abundances in these analyses therefore represent the intact, uningested component of *Syn* export, but might be overestimates if vortexing led to release of some fecal pellet *Syn*, or underestimates if *Syn* remained contained in sticky aggregates. EPI subsamples were stained with DAPI and proflavin and filtered onto 8-μm pore-size black Nuclepore filters. The filters were mounted on slides, and 30 positions from each slide were imaged at 200X in Z-stack mode with a Zeiss inverted epifluorescence microscope. Diatoms and other microplankton were identified and sized using ImagePro, and converted to carbon equivalents as described above for water-column samples. Recognizable tintinnids were excluded from the total microplankton counts.

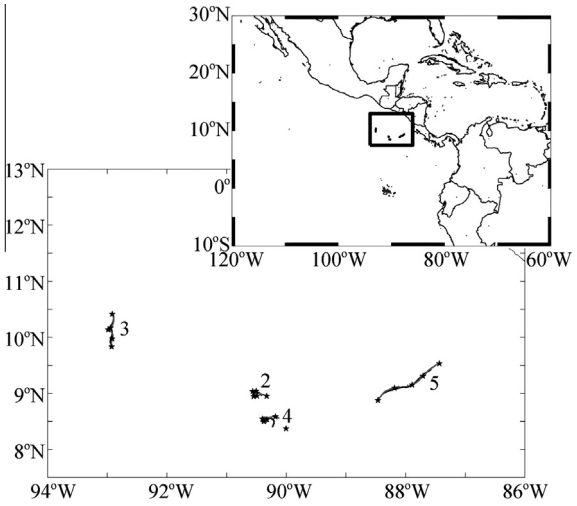

Fig. 1. Study region. Upper right panel shows study region within the greater western tropical Pacific. Black lines on main plot show the drifting sediment tracks for each cycle, while gray lines show the experimental array tracks. Often it is difficult to distinguish the two tracks at this scale as the two arrays tracked each other remarkably well. Black stars show the location of CTD casts.

3. Results

3.1. Study sites

Our Lagrangian cycles (Fig. 1) included two water parcels that were in the core of the CRD (Cycles 2 and 4), as visualized in enhanced surface Chl *a* in satellite images and in ADCP transect mapping of the flow field prior to the experimental work. Cycle 3 was located northeast of the core region, and Cycle 5 was closer to, and moving quickly toward, the coast. Intra-regional variability, however, was not pronounced. Mean surface temperature varied from 27.5 to 28.2 °C, with relatively shallow mixed layers of ~15 m followed closely by a strong thermocline that extended to depths of 40–50 m (Fig. 2a). Cycles 2–4 had very similar Chl *a* profiles (Fig. 2b) with surface values of ~0.25 μg L^{-1} and a 30-m deep chlorophyll max (DCM), while Cycle 5 had distinctly lower surface Chl *a* (0.19 μg L^{-1}) and higher Chl *a* at depth (50-m DCM). *Syn* concentrations were surface enhanced (Fig. 2c), with Cycle 2 containing the highest surface concentrations (2.1×10^5 cells mL^{-1}) and Cycle 5 the least (4.7×10^4 cells mL^{-1}).

3.2. Converting pigment measurements to cells and carbon

Our measurements of pigment fluxes into sediment traps and mesozooplankton guts integrate cells over a water column in which pigment:cell and pigment:carbon ratios vary with depth (Fig. 3b and d). In order to convert PE measurements to carbon measurements for direct comparison to the carbon fluxes measured in the sediment traps, we derived mean conversions by plotting <20-μm PE against *Syn* concentrations and forcing a linear regression through the origin (Fig. 3a). The mean regression result (6.4 fg PE $cell^{-1}$) is driven mainly by values in the upper to mid-euphotic zone, where *Syn* abundances were highest (Fig. 2). Ratios are higher in the lower euphotic zone, which is closest spatially to the depth of the sediment traps. Similarly, regressing phytoplankton C biomass from combined FCM and microscopy against Chl *a* estimates from the same hydrocasts, we estimated a mean water-column C:Chl ratio of 73. This ratio is intermediate between higher values in the upper euphotic zone and lower values in the deeper layer (Fig. 3d).

3.3. Sediment trap fluxes

Measured vertical fluxes for the four cycles (Table 2) ranged from 50.3 to 72.4 mg C m^{-2} d^{-1} at the base of the euphotic zone. At 150 m, fluxes ranged from 45.9 to 61.7 mg C m^{-2} d^{-1}, suggesting that roughly 15% of the sinking material was remineralized in the first 60 m directly below the euphotic zone.

Pigment fluxes displayed similar patterns but were more variable (Table 2). Phaeo flux ranged from 377 to 1368 μg Chl *a* equivalents m^{-2} d^{-1} at the base of the euphotic zone (90 m), with

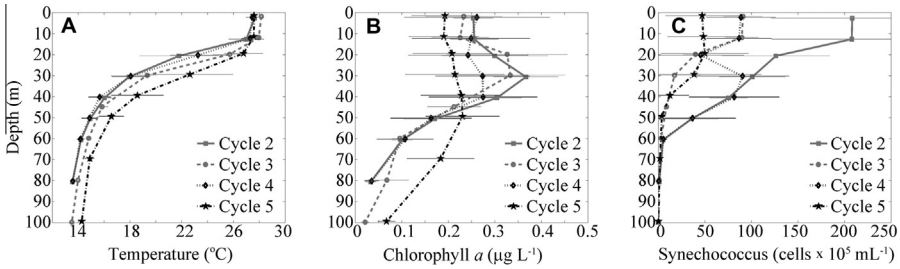

Fig. 2. Vertical profiles of temperature (A), Chl *a* (B), and *Syn* (C) for each cycle. Means of 5 CTD profiles are shown as well as standard deviations for each measurement. Although measurements were typically made at the same depths for each cycle, they are plotted with a slight vertical offset to increase visibility of error bars.

roughly 24% degraded before reaching 150-m depth. Chl *a* was not detected in three of the eight traps and only registered as a significant amount of the pigment flux on Cycle 5, where the Chl *a*: Phaeo export ratio was still <0.1 at 90 m. The export pattern for PE was similar to Phaeo, with a regression of PE on Phaeo explaining 84% of the variability in PE flux (Fig. 4). The small intercept suggests that the two pigments are transported to depth in relatively constant proportion (geometric mean = 0.04 μg PE:μg Phaeo), implying a common mechanism of export.

Based on our mean conversion estimate of 6.4 fg PE per *Syn* cell, the PE fluxes into sediment traps are equivalent to total export of 3.3×10^9 to 9.8×10^9 *Syn* cells $m^{-2}\,d^{-1}$ (Phyco*, Table 2). Since vertically integrated standing stocks ranged from 9.0×10^{11} to 7.4×10^{12} m^{-2} (with peak cycle concentrations of 5.0×10^4 to 2.8×10^5 L^{-1}), total *Syn* export marked by a pigment tracer signal ranged from 0.04% to 1.06% of standing stock per day. From FCM measurements, estimates of *Syn* export as individually recognizable cells were almost an order of magnitude lower (Table 2), suggesting that most *Syn* export tracked by the PE pigment arrived in fecal pellets or aggregates that were not easily disrupted by the vortexing and 200-μm pre-screening that was done prior to FCM analysis of the trap material.

Export of recognizable diatom cells in sediment trap material was uniformly low, never exceeding 0.5 mg C $m^{-2}\,d^{-1}$, and typically far less than that. The dominant diatoms in the sediment trap were small pennates with linear dimensions of roughly 20 μm × 3 μm, although larger pennate diatoms were responsible for most of the diatom flux in Cycle 5. Export of other microplankton (which were not identified to taxa but comprised mostly of a mixed community of flagellates) varied from 0.65 to 1.81 mg C $m^{-2}\,d^{-1}$ at the base of the euphotic zone. Overall, the flux of microscopically identifiable microplankton was of the same magnitude as the phytoplankton mass flux inferred from Chl *a* in the traps, which ranged from 0 to 9 mg C $m^{-2}\,d^{-1}$ assuming C:Chl = 73.

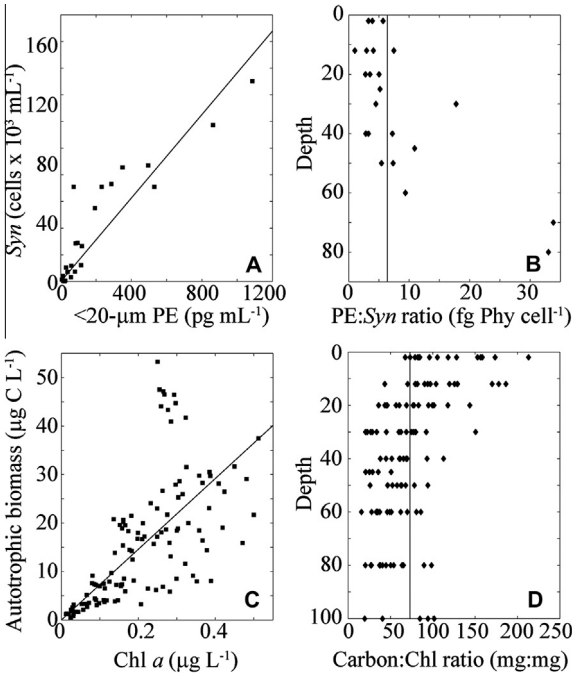

Fig. 3. Pigment ratios. Panel A shows the relationship between water column <10-μm phycoerythrin (PE) and *Synechococcus* (*Syn*) cell abundances (*y*-axis). The line shows the regression forced through the axis which equates to a PE:*Syn* ratio of 258 fg PE $cell^{-1}$. Panel B shows the PE:*Syn* ratio (*x*-axis) as a function of depth (*y*-axis). The plotted line is our calculated mean ratio of fg phycoerythrin $cell^{-1}$. Off the axes (and not plotted) is a value of 222 fg PE $cell^{-1}$ at a depth of 90 m, which was near the detection limit for PE and had only 95 *Syn* cells mL^{-1}. Panel C shows the relationship between autotrophic biomass (determined by epifluorescence microscopy and FCM; A.G. Taylor and K.E. Selph, unpub.) and Chl *a*. Line is the regression forced through zero, which equates to a C:Chl ratio of 73 mg:mg. Panel D shows the Chl:carbon ratio vs. depth, with a line showing our computed mean C:Chl of 73 mg:mg.

3.4. Grazing rate measurements

Despite the common perception that picoplankton cells are too small to be grazed by typical mesozooplankton, we found significant PE concentrations in our measurements of mesozooplankton gut contents (Table 3). Grazing rates varied from 0.23 to 0.36 mg PE $m^{-2}\,d^{-1}$, equivalent to 3.7×10^{10} to 5.8×10^{10} *Syn* cells $m^{-2}\,d^{-1}$. Mesozooplankton fecal pellets thus can easily account for the average of 0.04 mg PE $m^{-2}\,d^{-1}$ exported out of the euphotic zone. Intact *Syn* cells were also observed individually and in clumps within the fecal pellets of live mesozooplankton incubated in shipboard grazing experiments (Fig. 5), consistent with previous reports that they may not be significantly digested in passing through the guts of metazoan consumers (Silver and Bruland, 1981; Johnson et al., 1982; Gorsky et al., 1999). In calculations below, we assume that all direct consumption of *Syn* cells by mesozooplankton passed intact (i.e. without pigment degradation) through their digestive systems and into their fecal pellets (e.g. Gorsky et al., 1999).

Phaeo concentrations (indicative of grazing on Chl *a*), were high in the mesozooplankton gut analyses (2.08–7.53 mg Chl *a* equiv. $m^{-2}\,d^{-1}$; Table 3), suggesting substantial grazing pressure of 12–44% of Chl *a* standing stock d^{-1} by the mesozooplankton community. When compared to Phaeo fluxes measured in traps at the base of the euphotic zone (Table 2), 74–84% of the Chl *a* consumed by mesozooplankton disappeared between ingestion and export from the euphotic zone (either degraded in the guts of mesozooplankton or lost to disintegration/recycling of fecal pellets during sinking). A similar comparison of PE grazing to PE vertical flux indicates comparable loss rates of 75–92% of PE consumed. The similarity in these estimates, coupled with the fact that sediment trap PE appeared to be largely associated with transport of intact *Syn* cells in pellets, suggests that physical disintegration and/or recycling of pellet contents during euphotic zone transit

Table 2
Export fluxes of carbon, nitrogen, pigments and cells into sediment traps. All data are integrated over the depth interval shown (depth, m) in Column 1. Shown are: Chlorophyll *a* (Chl *a*, μg m^{-2} d^{-1}), Phaeo (phaeopigments, μg Chl *a* equiv m^{-2} d^{-1}), PE (phycoerythrin, μg m^{-2} d^{-1}), PE* (*Syn* abundance as calculated by multiplying PE flux by *Syn*:PE ratio, cells m^{-2} d^{-1}), SYN (*Syn* abundance as measured by FCM (flow cytometry), cells m^{-2} d^{-1}), phytoplankton biomass (mg C m^{-2} d^{-1}) measured by epifluorescence microscopy (diatoms, other micro), and Mass Flux of Carbon and Nitrogen (mg C or mg N m^{-2} d^{-1}) measured by combustion analysis. Values are mean ± standard error.

Cycle, depth, date (2010)	Pigments				FCM	EPI MICRO		Mass flux	
	Chl *a*	Phaeo	PE	PE*	*Syn*	Diatoms	Other Micro	Carbon	Nitrogen
C2, 90, July 4–8	0 ± 1.2	377 ± 40	20.4 ± 0.5	3.19×10^9	$3.52 \times 10^8 \pm 1.3 \times 10^7$	0	1.28	63.9 ± 18.3	7.4 ± 0.9
C2, 150	1.2 ± 2.7	270 ± 23	21.4 ± 17.0	3.35×10^9	$4.95 \times 10^8 \pm 6.9 \times 10^7$	0.003	0.44	50.7 ± 7.3	6.5 ± 0.3
C3, 90, July 9–13	21.2 ± 8.7	1219 ± 55	48.8 ± 15.3	7.63×10^9	$1.12 \times 10^9 \pm 1.7 \times 10^8$	0.007	1.7	67.3 ± 2.6	7.9 ± 0.2
C3, 150	2.7 ± 5.3	1024 ± 27	32.6 ± 7.0	5.11×10^9	$8.15 \times 10^8 \pm 9.1 \times 10^7$	0.006	1.11	55.3 ± 1.6	5.6 ± 0.6
C4, 90, July 15–19	0 ± 19.7	846 ± 105	25.5 ± 5.9	3.99×10^9	$6.34 \times 10^8 \pm 2.7 \times 10^7$	0.034	0.65	50.3 ± 2.8	6.0 ± 0.3
C4, 150	0 ± 0	529 ± 55	19.2 ± 9.4	3.01×10^9	$4.70 \times 10^8 \pm 1.6 \times 10^7$	0	1.1	45.9 ± 1.8	4.8 ± 0.2
C5, 90, July 20–23	122.6 ± 11.3	1368 ± 96	60.7 ± 7.6	9.50×10^9	$5.71 \times 10^8 \pm 8.4 \times 10^7$	0.43	1.81	72.4 ± 2.7	9.5 ± 0.4
C5, 150	51.6 ± 6.4	1166 ± 86	48.7 ± 7.8	7.62×10^9	$4.84 \times 10^8 \pm 1.5 \times 10^7$	0.073	1.95	61.7 ± 2.0	7.5 ± 1.1

was the most likely explanation for the low fraction of mesozooplankton pellets sinking into the traps.

Vertically integrated estimates of protozoan grazing on the total phytoplankton community from dilution experiments were roughly equivalent to mesozooplankton grazing for Cycles 3 and 5, and close to double mesozooplankton grazing estimates for Cycles 2 and 4 (Table 3). Protozoan grazing rates on Chl *a* averaged 54% of growth rates, based on the geometric mean of the dilution results. When only grazing on *Syn* cells was considered, however, the results were strikingly different. Protozoan grazing pressure on *Syn* was roughly 50 times higher than the direct mesozooplankton grazing pressure on *Syn* suggested by PE gut content measurements. Protozoan grazing alone was able to account for the average loss of 127% of *Syn* production estimates in our experimental incubations (Fig. 6).

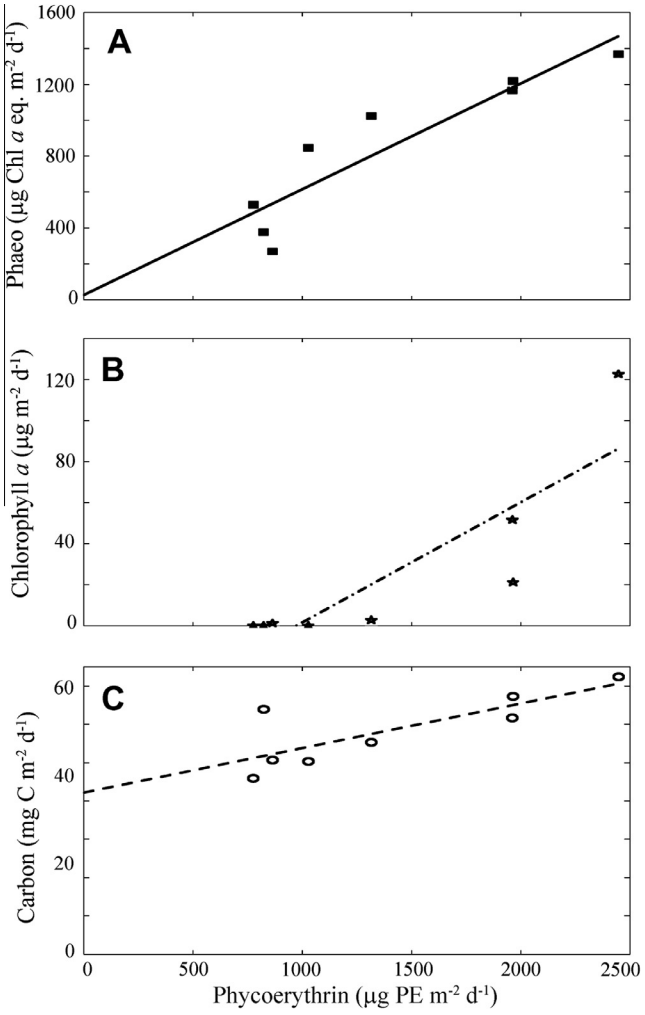

Fig. 4. Correlation of phycoerythrin (PE) flux with phaeopigment flux (Panel A), Chl *a* flux (B), and mass (carbon) flux (C). Solid line is the regression of Phaeo against PE (Phaeo = 27 + 0.59 × PE, $r^2 = 0.84$) and was the only regression for which the intercept was not significantly different from zero. Dashed-dotted line is the regression of Chl *a* against PE (Chl = −57 + 0.059 × PE, $r^2 = 0.75$). Dashed line is the regression of carbon against PE (C = 42 + 0.012 × PE, $r^2 = 0.64$). The regression of *Syn* flux (measured by FCM) against PE flux (not shown) was not significant.

4. Discussion

4.1. Ecosystem pathways of vertical flux

Our experiments were designed to generate comparable contemporaneous estimates of export fluxes for *Syn* and for total phytoplankton (including picoplankton) by three distinct pathways: direct sinking of ungrazed cells, sinking of unassimilated *Syn* and phytoplankton carbon in mesozooplankton fecal pellets, and indirect trophic transfer of *Syn* and total phytoplankton production via protozoan grazers to mesozooplankton. Interpretations of results hinge on several assumptions about carbon:pigment ratios and the resistance of pigments to conversion to non-fluorescent material that are discussed below. However, by making consistent assumptions for PE and the Chl *a*-Phaeo pigment pair (see bottom line of Table 1), we can create from the measured rates a robust budget for sinking material.

The contribution of ungrazed *Syn* to vertical flux is determined by multiplying FCM-derived cell flux by the *Syn* cellular carbon content (101 fg C; Garrison et al., 2000).

$$\text{Export}_{\text{ungrazed}} = \text{sedTrapSyn}_{\text{FCM}} \times 101 \text{ fg C cell}^{-1} \quad (2)$$

This varies from 0.03 to 0.11 mg C m^{-2} d^{-1} at the base of the euphotic zone, accounting for approximately 0.11% of total carbon flux (Table 4). The contribution of total unassimilated *Syn* can likewise be calculated by dividing vertical PE flux by our measured PE:*Syn* ratio (6.4 fg PE $cell^{-1}$) and multiplying by the *Syn* cellular carbon content:

$$\text{Export}_{\text{unassimilated}} = \text{SedTrapPE} \times \frac{\text{cells}}{\text{PE}} \times 101 \text{ fg C cell}^{-1} \quad (3)$$

This flux, which we attribute primarily to *Syn* carbon transported as intact cells in fecal pellets, varies from 0.32 to 0.95 mg C m^{-2}. If we subtract the contribution of *Syn* carbon (and PE) known to be from ungrazed cells, the direct transport of *Syn* carbon in fecal pellets averages 0.84% of total flux.

To estimate the amount of vertical flux supported by protozoan grazing on *Syn*, we first compute the total protozoan production

Table 3
Mesozooplankton and protozoan grazing rates. Mesozooplankton grazing rates are shown as Chl *a* (phaeopigments, Phaeo) or phycoerythrin (PE) in units of mg m^{-2} d^{-1}. PE* denotes the PE grazing converted to a cell-based *Syn* grazing (cells m^{-2} d^{-1}) using the regression in Fig. 3. Protozoan grazing rates are derived from vertically integrated microzooplankton dilution experiment results, for the entire community as Chl *a* (mg Chl *a* m^{-2} d^{-1}) and for *Syn* (cells m^{-2} d^{-1}). The final two columns are the equivalent phytoplankton production rates measured by the dilution technique for the entire community (Chl *a*, mg m^{-2} d^{-1}) and for *Syn* (cells m^{-2} d^{-1}). Values are mean ± standard error.

Cycle	Mesozooplankton			Protozoan		Production	
	Phaeo	PE	PE*	Chl *a*	*Syn*	Chl *a*	*Syn*
2	2.08 ± 0.33	0.27 ± 0.08	4.24×10^{10}	5.7 ± 0.4	$4.89 \times 10^{12} \pm 5.5 \times 10^{11}$	9.2 ± 0.8	$3.33 \times 10^{12} \pm 6.3 \times 10^{11}$
3	7.53 ± 1.55	0.36 ± 0.07	5.67×10^{10}	7.2 ± 2.3	$1.72 \times 10^{12} \pm 9.0 \times 10^{10}$	12 ± 2.0	$1.18 \times 10^{12} \pm 9.7 \times 10^{10}$
4	3.2 ± 0.42	0.23 ± 0.10	3.55×10^{10}	5.9 ± 1.3	$2.58 \times 10^{12} \pm 3.0 \times 10^{11}$	11.5 ± 1.8	$2.35 \times 10^{12} \pm 1.8 \times 10^{11}$
5	7.29 ± 043	0.24 ± 0.04	3.76×10^{10}	6.4 ± 1.2	$9.72 \times 10^{11} \pm 4.1 \times 10^{11}$	14.2 ± 1.4	$8.97 \times 10^{11} \pm 1.7 \times 10^{11}$

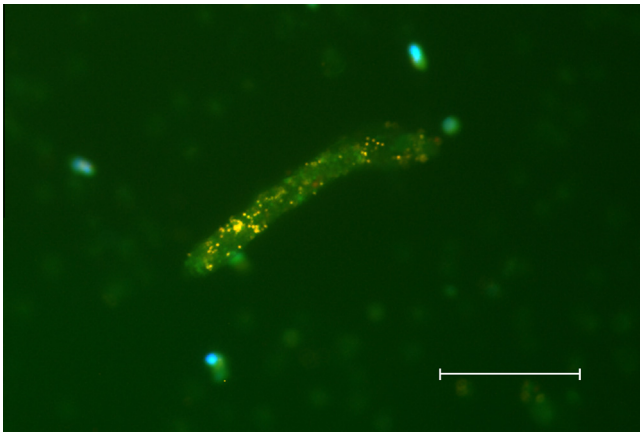

Fig. 5. Epifluorescence image of a euphausiid fecal pellet produced during feeding experiments at sea (data not shown, from separate experiments conducted by M. Decima on this cruise). The sample was stained with proflavin (protein stain) and DAPI (DNA stain), then mounted on a black filter and excited with blue (450–490 nm) light and UV (340–380 nm) light. With this preparation, proflavin staining imparts a green fluorescence to proteins, allowing the edge of the fecal pellet to be visualized, and orange fluorescence is from naturally-fluorescing phycoerythrin in *Synechococcus* cells. Scale bar is 50 μm.

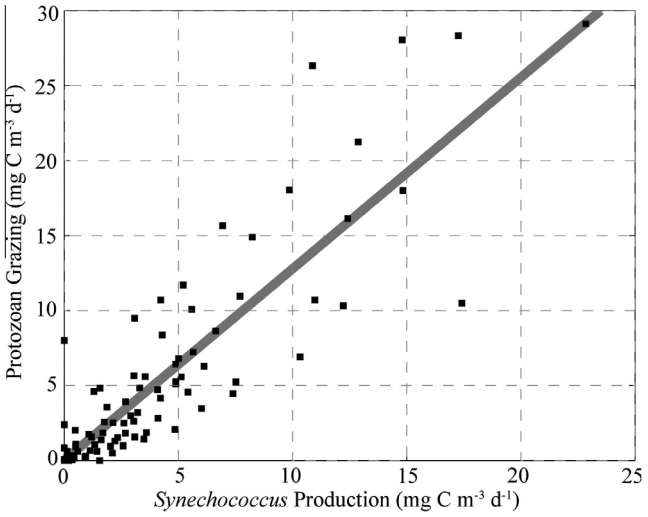

Fig. 6. *Syn* production (*x*-axis) and protozoan grazing on *Syn* (*y*-axis) as measured by the microzooplankton dilution technique. Solid line is the regression of grazing against growth (grazing = 1.28 × growth + 0.02, R^2 = 0.84).

based on grazing of *Syn* that is available to mesozooplankton as the product of protozoan grazing on *Syn* (Table 3) and an assumed protozoan gross growth efficiency of 30% (Straile, 1997):

$$\text{Production}_{\text{protozoa}} \leqslant \text{Gr}_{\text{protozoa}-Syn} \times \text{GGE}_{\text{protozoa}} \quad (4)$$

(Note that the above equation is an inequality, as it assumes only one protozoan trophic step between *Syn* and mesozooplankton. Additional trophic steps within the protozoa – grazing of protozoans on protozoans – would decrease the total production available to mesozooplankton, see Section 4.2.) We then estimate the fraction of this carbon that is lost by pellet remineralization before sinking out of the base of the euphotic zone by comparing the pigments consumed by mesozooplankton (Phaeo and PE, Table 3) to the pigment fluxes measured in the sediment traps (Table 2):

$$\text{Remineralization} = 1 - \frac{\text{Pigment}_{\text{sedtrap}}}{\text{Pigment}_{\text{mesozoo}}/\text{CE}} \quad (5)$$

where CE is the conversion efficiency of pigment to non-fluorescent molecules within mesozooplankton guts. For the Chl *a*/phaeopigment pair, Durbin and Campbell (2007) have shown that the mesozooplankton gut evacuation calculations take into account the loss of pigments to non-fluorescent phaeophorbides, thus the quantity $\text{pigment}_{\text{mesozoo}}/\text{CE}$ is equivalent to the mesozooplankton grazing rate found in Table 3. For PE, CE = 1 for *Syn* cells that pass through mesozooplankton guts undigested. From these calculations we thus calculate remineralization for Phaeo as 74–84%, and 75–92% for PE. Assuming for each cycle that the carbon in sinking fecal pellets is lost proportionally to the mean loss rates of the two pigments and that only one trophic step separates *Syn* from mesozooplankton, we calculate an upper estimate of the proportion of vertical flux transported by *Syn* through mesozooplankton grazing on protozoans from:

$$\text{Export}_{\text{multiv}} \leqslant \text{Production}_{\text{protozoa}} \times \text{EE}_{\text{mesozoo}} \times (1 - \text{Remineralization}) \quad (6)$$

where $\text{EE}_{\text{mesozoo}}$ is the egestion efficiency of mesozooplankton (30%; Conover, 1966).

Across our four experimental cycles, this upper estimate for the multivorous export pathway averaged 5.6% of total flux. Upper limits for the total contributions of *Syn* to vertical flux at the base of the euphotic zone can thus be determined as 9.2%, 4.9%, 8.3% and 4.0%, respectively, for Cycles 2–5. Contributions of *Syn* to total primary production in the same water parcels are 50.2%, 13.6%, 28.2% and 8.7% (Table 4). *Syn* therefore contributes to export at disproportionately low rates (2–5-fold lower) compared to its contribution to production. The above contribution estimates of *Syn* to export may however be significant overestimates if longer trophic pathways separate *Syn* from mesozooplankton.

In a completely analogous way, we use pigment, microscopical- and FCM estimates of total phytoplankton biomass and rates to assess the contribution of total ungrazed phytoplankton to vertical flux, the export of Phaeo in herbivorous fecal pellets, and the role of fecal pellets in transporting carbon to depth via the indirect trophic pathway. The only difference between the equations for Chl *a* and PE, is that while we assume that *Syn* passes undigested through mesozooplankton guts, most of the total organic carbon

Table 4
Proportion of total and export production. First column shows the proportion of total primary production attributable to *Syn* as assessed by dividing the microzooplankton dilution-derived production rates of *Syn* by Chl *a* based production rates. Next four columns show the fraction of total export supported by total phytoplankton due to sinking of ungrazed cells, herbivorous fecal pellets (with the conservative assumption that CE = 1, see Eq. (7)), herbivorous fecal pellets* (with the more realistic assumption that CE = 0.45, see Section 4.2), and a potential upper estimate of mesozooplankton fecal pellets produced from grazing on protozoans. Final three columns show the equivalent proportion of export supported by *Syn* production through each of those three pathways. For more details see Section 4.1.

Cycle	Depth	Production	Export supported by total Phyto				Export supported by *Syn*		
		% PrimProd supported by *Syn*	Sinking of ungrazed micro-plankton (% total POC export)	Fecal pellets (Herbiv.) (% total POC export)	Fecal pellets (Herbiv*) (% total POC export)	Fecal pellets (Trophic transfer) (% total POC export)	Sinking of ungrazed *Syn* (% total POC export)	Fecal pellets (Herbiv.) (% total POC export)	Fecal pellets (Trophic transf.) (% total POC export)
2	90	50.2	2.00	12.9	28.7	7.5	0.06	0.45	8.71
	150	–	0.87	11.7	26.0	7.7	0.10	0.57	8.95
3	90	13.6	2.53	39.7	88.2	10.5	0.17	0.98	3.79
	150	–	2.02	40.6	90.2	9.7	0.15	0.79	3.52
4	90	28.2	1.36	36.8	81.7	14.4	0.13	0.67	7.49
	150	–	2.39	25.2	56.0	10.5	0.10	0.56	5.45
5	90	8.7	3.09	41.4	92	12.8	0.08	1.25	2.66
	150	–	3.28	41.4	92	12.3	0.08	1.17	2.57

ingested by mesozooplankton is subject to digestion and absorption during gut passage. Thus, Eq. (3) is rewritten as:

$$\text{Export}_{\text{unassilimated}} = \text{SedTrapPhaeo} \times \text{C} : \text{Chl}_{\text{phyto}} \times \frac{\text{EE}_{\text{mesozoo}}}{\text{CE}} \qquad (7)$$

where as before $\text{EE}_{\text{mesozoo}}$ is the egestion efficiency of the mesozooplankton and CE is the conversion efficiency of Chl *a* to phaeo (instead of non-fluorescent molecules). We again assume that $\text{EE}_{\text{mesozoo}} = 0.3$, and further make the conservative assumption that CE = 1 (but see Section 4.2). These calculations indicate that 2.2% of total carbon flux is attributable to ungrazed phytoplankton on average, 32.7% arrives as herbivorous grazing byproducts in fecal pellets, and 11.3% is transferred via the indirect trophic transfer pathway (Table 4). By this accounting, the use of Chl *a* as a grazing tracer accounts for a little less than half of the total carbon exported from the euphotic zone. However, it is worth noting that this may be due to our conservative estimate of the flux of herbivorous fecal pellets. Nevertheless, it is clear that fecal pellets of suspension feeding mesozooplankton constitute a dominant mechanism of export flux from the euphotic zone.

4.2. Sensitivity to assumptions

As Fig. 3b and d makes clear, pigment:carbon ratios are not constant in the ocean, but typically increase with depth. Our decision to use average pigment:carbon ratios from a linear regression of biomass on pigment assumes that the depth strata with maximum biomass contribute most to mass fluxes (especially grazing). The bead-normalized PE fluorescence per *Syn* cell determined from FCM analyses of sediment trap samples was, in fact, similar to that measured in water-column samples from ~50 m, suggesting that our estimate of 6.4 fg PE cell^{-1} for sinking *Syn* was reasonable.

While our pigment:carbon ratios in the water column seem robust, another site of decoupling of the pigment to carbon ratio is within mesozooplankton guts. *Syn* cells likely pass through mesozooplankton guts intact and even if they are degraded, PE (a protein) is likely digested at a similar rate to total *Syn* carbon. However, the equivalence of ingested and egested pigment:carbon ratio is unlikely to be true for total phytoplankton. It is important to note that our assumption of CE = 1 (the conversion efficiency of Chl *a* to phaeo) in Eq. (7) may lead to a large underestimate of the herbivorous fecal pellet pathway (but not the herbivorous pathway for *Syn*, where we assumed that CE = EE, Eq. (3)). While early studies assumed that Chl *a* was quantitatively converted to phaeopigments (Downs and Lorenzen, 1985), it has since been shown that the fraction of Chl *a* converted to non-fluorescent particles can be highly variable (Conover et al., 1986; Dagg and Walser, 1987; Penry and Frost, 1991). Goericke et al. (2000) measured the conversion of Chl *a* to non-fluorescent phaeophorbides (1-CE, in our Eq. (7)), and found it to range from 40% to 70%. For a more accurate estimate of the C:Phaeo ratio within fecal pellets, we could, rather than assuming that the C:pigment ratio remains constant as material passes through the gut, take the midpoint of the Goericke et al. (2000) measurements (CE = 45%) while still assuming 70% assimilation efficiency of carbon. In this case, the C:Phaeo ratio of herbivorous fecal pellets, and hence their contribution to flux, would increase by a factor of (1/CE) = 2.2. While this affects the herbivorous pathway for total phytoplankton, altered estimates of CE will not alter export estimates of the trophic transfer pathway, since the true (but unknown) CE is taken into account in typical mesozooplankton gut evacuation experiments (Durbin and Campbell, 2007). Under the aforementioned assumption of CE = 0.45, the percent total contribution of *Syn* production to export would remain 9.2%, 4.9%, 8.3% and 4.0% for Cycles 2–5, respectively, but the percent contribution of total phytoplankton production to export would be 38.2%, 101.1%, 97.5%, and 107.8%, which is remarkably good agreement for three of our four water parcels.

That export was predominantly supported by mesozooplankton fecal pellet production is further supported by the measured balance of growth and grazing in our experiments. According to the Chl-based rate estimates in Table 3, the mean (±s.d.) difference between total phytoplankton community production and consumption by protozoans is 5.4 ± 1.8 mg Chl equiv. m^{-2} d^{-1}). The fact that this is statistically indistinguishable from the estimated rate of mesozooplankton grazing (5.0 ± 2.8 mg Chl equiv. m^{-2} d^{-1}) indicates that phytoplankton production was balanced by total grazing pressure, leaving little excess production available for direct export. Using these same methods and assumptions, similar production-grazing balances have also been described for the HNLC equatorial region from a large data set of many stations (Landry et al., 2011).

The assumption of greatest importance to our calculation of the total contribution of *Syn* to export is that made to calculate the magnitude of indirect trophic transfer from protozoan grazing, since this is, according to our results, the pathway that transports the most *Syn*-generated production to depth. The most conservative guess is that a single protozoan trophic step separates *Syn* from mesozooplankton. While a wide range of grazers is known to feed on *Syn* (Caron et al., 1991; Jeong et al., 2005; Frias-Lopez et al., 2009), the dominant grazers of picoplankton in both

oligotrophic and upwelling regions of the open ocean are <5-μm protozoans (Calbet and Landry, 1999; Christaki et al., 2001; Sherr and Sherr, 2002). Considering that much larger cells like diatoms are also subject to high rates of protozoan grazing in the open ocean (Landry et al., 2011), it could well be that the nanoflagellate predators of *Syn* are in turn the prey of other protozoans. Assuming 30% gross growth efficiencies for each trophic step separating *Syn* from mesozooplankton decreases the contribution of the indirect trophic transfer pathway to flux by 70%. Two protozoan trophic steps would result in total *Syn* contributions to export ranging from 2.1% to 3.1%, while three steps would reduce their composite contributions to only 1.3–1.6% of vertical carbon flux. It is thus clear that the assumption of one protozoan trophic step gives an upper limit for *Syn* contribution to export flux. The minimum estimate (~1%) is the amount directly measured by PE flux into sediment traps.

4.3. The role of picophytoplankton in vertical flux

Based on inverse model analysis, Richardson and Jackson (2007) argued that picophytoplankton dominated vertical carbon export in the open ocean and that the mechanism was primarily through aggregation and sinking of ungrazed cells. However, if picophytoplankton production is almost entirely consumed by protozoan grazers as in the present experiments and many others (Latasa et al., 1997; Selph et al., 2011), ungrazed cells seem unlikely to be the major export mechanism. Indeed, further results of inverse analyses with better constraints on size-structured production and grazing rates, have indicated significant, though not dominant, contributions of picophytoplankton-derived production to export, but mainly through indirect trophic transfers after initial grazing (Stukel and Landry, 2010).

Our present field results indicate that direct flux of ungrazed picophytoplankton (as measured flow cytometrically) was a negligible component of both total carbon export and picophytoplankton loss from the euphotic zone. While it is possible that the greater *Syn* export estimates suggested by PE concentrations in the sediment traps may have originated from robust aggregates that resisted our disruption approach (vortexing), the strong similarity between the percentages of mesozooplankton-ingested Phaeo and PE reaching the sediment traps (Fig. 4) suggests that most PE was transported in fecal pellets. While direct grazing of mesozooplankton on *Syn* cells was a small loss term for picophytoplankton in our experiments, its impact on export of *Syn* (Table 3) was two orders of magnitude higher than direct cell sinking (Table 2). The primary role of aggregation may be to make picophytoplankton available to mesozooplankton (Wilson and Steinberg, 2010), rather than to catalyze sinking directly. Aggregation may still play a role in export, however, if pellets are transported in association with aggregates, or if pellets degrade to amorphous aggregates.

Appendicularians, salps and large pyrosome colonies, all capable of feeding directly on small particles, were abundant at various times during our experiments in the CRD, so metazoan grazing cannot be ruled out as an important mechanism for cell concentration and aggregation, such as the uningested cells in discarded appendularian houses. Our observations – the presence of abundant intact *Syn* cells in fecal pellets and evidence that most pellets never leave the euphotic zone – also raise intriguing possibilities that *Syn* can benefit in some ways from being in fecal pellets (e.g. enhanced nutrient environment and protection from protozoan grazers) and that the cells in disintegrating pellets may be repeatedly cycled by mesozooplankton. We note that even in the early days of microbial loop discoveries, Johnson et al. (1982) envisioned viable intact *Syn* cells being transported to great ocean depth in the fecal pellets of large grazers. While our results stop at 150-m deep sediment traps, they are consistent with this mechanism of picophytoplankton delivery to greater ocean depths.

While this is only a single study, our conclusions are in agreement with data from other sites. Picophytoplankton and their diagnostic pigments are frequently found in sediment traps (Rodier and Le Borgne, 1997; Waite et al., 2000; Lamborg et al., 2008), as suspended particulates in the mesopelagic zone (Lomas and Moran, 2011; Sohrin et al., 2011), and even in deep-sea sediments (Lochte and Turley, 1988; Pfannkuche and Lochte, 1993). Nevertheless, when the carbon transported by these cells has been directly measured and compared to concurrent total POC flux, it has typically accounted for a minor (on the order of 0.1%) proportion of sediment trap flux (Turley and Mackie, 1995; Rodier and Le Borgne, 1997; Waite et al., 2000). Using water-column pigments and ^{234}Th measurements, Lomas and Moran (2011) estimated that the cyanobacteria contribution to export was an order of magnitude less than their contribution to biomass, although still a significant 5% each for *Syn* and *Prochlorococcus*. Their study assumed, however, that the contribution of pigments to sinking flux was equal to their contribution to standing stocks in the mesopelagic. The growing evidence that picocyanobacteria production is balanced by protozoan grazing in the open ocean (Liu et al., 2002; Hirose et al., 2008; Selph et al., 2011) also suggests that little picophytoplankton production remains for direct export. In addition, the low export efficiency (*e*-ratio = export/^{14}C-PP was ~5%) in the picophytoplankton-dominated CRD is consistent with other studies that find high ratios associated with communities dominated by diatoms and large phytoplankton (Buesseler, 1998; Buesseler et al., 2008). Nevertheless, we find that picophytoplankton may contribute significantly to export through protozoan grazing pathways that link them to mesozooplankton. Constraining the number of trophic transfers within the protozoan grazer chain therefore remains an important step toward accurately linking the production of plankton size classes to biogeochemical fluxes.

5. Conclusions

Despite variability in the contribution of *Syn* to biomass and primary production, several robust patterns emerged from four water parcels studied in the CRD. While *Syn* contributed greatly to total primary production (25% of PP, varying from 9% to 50%), its direct contribution to export flux was negligible. PE measurements suggested that unassimilated *Syn* did not exceed 1.25% of total POC export into sediment traps at the base of the euphotic zone, and based on a comparison to FCM-derived *Syn* flux estimates (an order of magnitude lower) and high PE concentrations in mesozooplankton guts, we attribute most of this direct flux to transport of undigested *Syn* in mesozooplankton fecal pellets. In contrast to the direct flux of unassimilated *Syn* carbon, the export supported indirectly by *Syn* may be considerably higher. Protozoa consumed most, close to all, of *Syn* production. Depending on assumptions about the gross growth efficiency of protozoa and the mean number of protozoan trophic steps, the trophic pathway from *Syn* through protozoa to mesozooplankton fecal pellets contributed 0.5–6.6% of total POC flux. Given the order-of-magnitude uncertainty in this multivorous transport pathway, determining the efficiency of the protozoan link is thus critical for assessing the total contribution of *Syn* to export. Despite this uncertainty, comparison of the PE and Chl *a* budgets clearly shows that most export in the CRD is associated with herbivorous mesozooplankton fecal pellets.

Acknowledgments

We thank the captain, crew, and restechs of the R/V Melville, our home away from home. We are grateful to all of our colleagues

in the Flux and Zinc Experiments (FLUZiE) Program, particularly Joachim Goes, Andrés Gutiérrez, C.J. Bradley, Ally Pasulka, Andrew Taylor, Dan Wick and John Wokuluk for their help at sea and in the lab, and to three anonymous reviewers for their insightful comments. This work was supported by National Science Foundation (NSF) Grant OCE-0826626 and by a National Aeronautics and Space Administration, Earth and Space Science fellowship to M. Stukel.

References

Amacher, J., Neuer, S., Anderson, I., Massana, R., 2009. Molecular approach to determine contributions of the protist community to particle flux. Deep-Sea Research I 56, 2206–2215.

Brown, S.L., Landry, M.R., Barber, R.T., Campbell, L., Garrison, D.L., Gowing, M.M., 1999. Picophytoplankton dynamics and production in the Arabian Sea during the 1995 Southwest Monsoon. Deep-Sea Research II 46, 1745–1768.

Buesseler, K.O., 1998. The decoupling of production and particulate export in the surface ocean. Global Biogeochemical Cycles 12, 297–310.

Buesseler, K.O., Trull, T.W., Steinber, D.K., Silver, M.W., Siegel, D.A., Saitoh, S.I., Lamborg, C.H., Lam, P.J., Karl, D.M., Jiao, N.Z., Honda, M.C., Elskens, M., Dehairs, F., Brown, S.L., Boyd, P.W., Bishop, J.K.B., Bidigare, R.R., 2008. VERTIGO (VERtical Transport in the Global Ocean): a study of particle sources and flux attenuation in the North Pacific. Deep-Sea Research II 55, 1522–1539.

Calbet, A., Landry, M.R., 1999. Mesozooplankton influences on the microbial food web: direct and indirect trophic interactions in the oligotrophic open ocean. Limnology and Oceanography 44, 1370–1380.

Caron, D.A., Lim, E.L., Miceli, G., Waterbury, J.B., Valois, F.W., 1991. Grazing and utilization of chroococcoid cyanobacteria and heterotrophic bacteria by protozoa in laboratory cultures and a coastal plankton community. Marine Ecology Progress Series 76, 205–217.

Christaki, U., Giannakourou, A., Van Wambeke, F., Gregori, G., 2001. Nanoflagellate predation on auto- and heterotrophic picoplankton in the oligotrophic Mediterranean Sea. Journal of Plankton Research 23, 1297–1310.

Conover, R.J., 1966. Assimilation of organic matter by zooplankton. Limnology and Oceanography 11, 338–345.

Conover, R.J., Durvasula, R., Roy, S., Wang, R., 1986. Probable loss of chlorophyll-derived pigments during passage through the gut of zooplankton, and some of the consequences. Limnology and Oceanography 31, 878–887.

Dagg, M.J., Walser, W.E., 1987. Ingestion, gut passage, and egestion by the copepod *Neocalanus plumchrus* in the laboratory and in the Subarctic Pacific Ocean. Limnology and Oceanography 32, 178–188.

Décima, M., Landry, M.R., Rykaczewski, R.R., 2011. Broad-scale patterns in mesozooplankton biomass and grazing in the eastern equatorial Pacific. Deep-Sea Research II.

Dore, J.E., Brum, J.R., Tupas, L.M., Karl, D.M., 2002. Seasonal and interannual variability in sources of nitrogen supporting export in the oligotrophic subtropical North Pacific Ocean. Limnology and Oceanography 47, 1595–1607.

Downs, J.N., Lorenzen, C.J., 1985. Carbon: pheopigment ratios of zooplankton fecal pellets as an index of herbivorous feeding. Limnology and Oceanography 30, 1024–1036.

Durbin, E.G., Campbell, R.G., 2007. Reassessment of the gut pigment method for estimating in situ zooplankton ingestion. Marine Ecology Progress Series 331, 305–307.

Fiedler, P.C., 2002. The annual cycle and biological effects of the Costa Rica Dome. Deep-Sea Research I 49, 321–338.

Frias-Lopez, J., Thompson, A., Waldbauer, J., Chisholm, S.W., 2009. Use of stable isotope-labelled cells to identify active grazers of picocyanobacteria in ocean surface waters. Environmental Microbiology 11, 512–525.

Garrison, D.L., Gowing, M.M., Hughes, M.P., Campbell, L., Caron, D.A., Dennett, M.R., Shalapyonok, A., Olson, R.J., Landry, M.R., Brown, S.L., Liu, H.B., Azam, F., Steward, G.F., Ducklow, H.W., Smith, D.C., 2000. Microbial food web structure in the Arabian Sea: a US JGOFS study. Deep-Sea Research II 47, 1387–1422.

Goericke, R., Strom, S.L., Bell, R.A., 2000. Distribution and sources of cyclic pheophorbides in the marine environment. Limnology and Oceanography 45, 200–211.

Gorsky, G., Chretiennot-Dinet, M.J., Blanchot, J., Palazzoli, I., 1999. Picoplankton and nanoplankton aggregation by appendicularians: fecal pellet contents of *Megalocercus huxleyi* in the equatorial Pacific. Journal of Geophysical Research – Oceans 104, 3381–3390.

Hirose, M., Katano, T., Nakano, S.I., 2008. Growth and grazing mortality rates of *Prochlorococcus*, *Synechococcus* and eukaryotic picophytoplankton in a bay of the Uwa Sea, Japan. Journal of Plankton Research 30, 241–250.

Jeong, H.J., Park, J.Y., Nho, J.H., Park, M.O., Ha, J.H., Seong, K.A., Jeng, C., Seong, C.N., Lee, K.Y., Yih, W.H., 2005. Feeding by red-tide dinoflagellates on the cyanobacterium *Synechococcus*. Aquatic Microbial Ecology 41, 131–143.

Johnson, P.W., Xu, H.S., Sieburth, J.M., 1982. The utilization of chroococcoid cyanobacteria by marine protozooplankters but not by calanoid copepods. Annales De L Institut Oceanographique 58, 297–308.

Kleppel, G.S., Pieper, R.E., 1984. Phytoplankton pigments in the gut contents of planktonic copepods from coastal waters off southern California. Marine Biology 78, 193–198.

Knauer, G.A., Martin, J.H., Bruland, K.W., 1979. Fluxes of particulate carbon, nitrogen, and phosphorus in the upper water column of the Northeast Pacific. Deep-Sea Research 26, 97–108.

Lamborg, C.H., Buesseler, K.O., Valdes, J., Bertrand, C.H., Bidigare, R., Manganini, S., Pike, S., Steinberg, D., Trull, T., Wilson, S., 2008. The flux of bio- and lithogenic material associated with sinking particles in the mesopelagic "twilight zone" of the northwest and North Central Pacific Ocean. Deep-Sea Research II 55, 1540–1563.

Landry, M.R., Brown, S.L., Rii, Y.M., Selph, K.E., Bidigare, R.R., Yang, E.J., Simmons, M.P., 2008. Depth-stratified phytoplankton dynamics in Cyclone Opal, a subtropical mesoscale eddy. Deep-Sea Research II 55, 1348–1359.

Landry, M.R., Haas, L.W., Fagerness, V.L., 1984. Dynamics of microbial plankton communities: experiments in Kaneohe Bay, Hawaii. Marine Ecology Progress Series 16, 127–133.

Landry, M.R., Ohman, M.D., Goericke, R., Stukel, M.R., Tsyrklevich, K., 2009. Lagrangian studies of phytoplankton growth and grazing relationships in a coastal upwelling ecosystem off Southern California. Progress in Oceanography 83, 208–216.

Landry, M.R., Selph, K.E., Taylor, A.G., Décima, M., Balch, W.M., Bidigare, R.R., 2011. Phytoplankton growth, grazing and production balances in the HNLC equatorial Pacific. Deep-Sea Research II 58, 524–535.

Latasa, M., Landry, M.R., Schluter, L., Bidigare, R.R., 1997. Pigment-specific growth and grazing rates of phytoplankton in the central equatorial Pacific. Limnology and Oceanography 42, 289–298.

Li, W.K.W., Rao, D.V.S., Harrison, W.G., Smith, J.C., Cullen, J.J., Irwin, B., Platt, T., 1983. Autotrophic picoplankton in the tropical ocean. Science 219, 292–295.

Liu, H.B., Suzuki, K., Saino, T., 2002. Phytoplankton growth, and microzooplankton grazing in the subarctic Pacific Ocean and the Bering Sea during summer 1999. Deep-Sea Research I 49, 363–375.

Lochte, K., Turley, C.M., 1988. Bacteria and cyanobacteria associated with phytodetritus in the deep sea. Nature 333, 67–69.

Lomas, M.W., Moran, S.B., 2011. Evidence for aggregation and export of cyanobacteria and nano-eukaryotes from the Sargasso Sea euphotic zone. Biogeosciences 8, 203–216.

Menden-Deuer, S., Lessard, E.J., 2000. Carbon to volume relationships for dinoflagellates, diatoms, and other protist plankton. Limnology and Oceanography 45, 569–579.

Michaels, A.F., Silver, M.W., 1988. Primary production, sinking fluxes and the microbial food web. Deep-Sea Research 35, 473–490.

Monger, B.C., Landry, M.R., 1993. Flow cytometric analysis of marine bacteria with Hoechst 33342. Applied and Environmental Microbiology 59, 905–911.

Penry, D.L., Frost, B.W., 1991. Chlorophyl *a* degradation by *Calanus pacificus*: dependence on ingestion rate and digestive acclimation to food resources. Limnology and Oceanography 36, 147–159.

Pfannkuche, O., Lochte, K., 1993. Open ocean pelago-benthic coupling: cyanobacteria as tracers of sedimenting salp feces. Deep-Sea Research I 40, 727–737.

Poulton, A.J., Holligan, P.M., Hickman, A., Kim, Y.N., Adey, T.R., Stinchcombe, M.C., Holeton, C., Root, S., Woodward, E.M.S., 2006. Phytoplankton carbon fixation, chlorophyll-biomass and diagnostic pigments in the Atlantic Ocean. Deep-Sea Research II 53, 1593–1610.

Richardson, T.L., Jackson, G.A., 2007. Small phytoplankton and carbon export from the surface ocean. Science 315, 838–840.

Rodier, M., Le Borgne, R., 1997. Export flux of particles at the equator in the western and central Pacific Ocean. Deep-Sea Research II 44, 2085–2113.

Saito, M.A., Rocap, G., Moffett, J.W., 2005. Production of cobalt binding ligands in a *Synechococcus* feature at the Costa Rica upwelling dome. Limnology and Oceanography 50, 279–290.

Selph, K.E., Landry, M.R., Allen, C.B., Calbet, A., Christensen, S., Bidigare, R.R., 2001. Microbial community composition and growth dynamics in the Antarctica Polar Front and seasonal ice zone during late spring 1997. Deep-Sea Research II 48 (19–20), 4059–4080.

Selph, K.E., Landry, M.R., Taylor, A.G., Yang, E.J., Measures, C.I., Yang, J.J., Stukel, M.R., Christenson, S., Bidigare, R.R., 2011. Spatially-resolved taxon-specific phytoplankton production and grazing dynamics in relation to iron distributions in the equatorial Pacific between 110 and 140°W. Deep-Sea Research II 58, 358–377.

Sherr, B.F., Sherr, E.B., 1993. Preservation and storage of samples for enumeration of heterotrophic protists. In: P.F. Kemp, P.F., Sherr, B.F., Sherr, E.B., Cole, J.J., (Eds.), Handbook of Methods in Aquatic Microbial Ecology. CRC-Press, 207–212.

Sherr, E.B., Sherr, B.F., 2002. Significance of predation by protists in aquatic microbial food webs. Antonie Van Leeuwenhoek International Journal of General and Molecular Microbiology 81, 293–308.

Silver, M.W., Bruland, K.W., 1981. Differential feeding and fecal pellet composition of salps and pteropods, and the possible origin of the deep-water flora and olive-green cells. Marine Biology 62, 263–273.

Silver, M.W., Gowing, M.M., 1991. The "particle" flux: origins and biological components. Progress in Oceanography 26, 75–113.

Sohrin, R., Isaji, M., Obara, Y., Agostini, S., Suzuki, Y., Hiroe, Y., Ichikawa, T., Hidaka, K., 2011. Distribution of *Synechococcus* in the dark ocean. Aquatic Microbial Ecology 64, 1–14.

Straile, D., 1997. Gross growth efficiencies of protozoan and metazoan zooplankton and their dependence on food concentration, predator-prey weight ratio, and taxonomic growth. Limnology and Oceanography 42 (6), 1375–1385.

Strickland, J.D., Parsons, T.R., 1972. A Practical Handbook of Seawater Analysis, second ed. Bulletin of the Fisheries Research Board of Canada, No. 167.

Stukel, M.R., Landry, M.R., 2010. Contribution of picophytoplankton to carbon export in the equatorial Pacific: a re-assessment of food-web flux inferences from inverse models. Limnology and Oceanography 55, 2669–2685.

Taylor, A.G., Goericke, R., Landry, M.R., Selph, K.E., Wick, D.A., Roadman, M.J., 2012. Sharp gradients in phytoplankton community structure across a frontal zone in the California Current Ecosystem. Journal of Plankton Research.

Turley, C.M., Mackie, P.J., 1995. Bacterial and cyanobacterial flux to the deep NE Atlantic on sedimenting particles. Deep-Sea Research I 42, 1453–1474.

Waite, A.M., Safi, K.A., Hall, J.A., Nodder, S.D., 2000. Mass sedimentation of picoplankton embedded in organic aggregates. Limnology and Oceanography 45, 87–97.

Wilson, S.E., Steinberg, D.K., 2010. Autotrophic picoplankton in mesozooplankton guts: evidence of aggregate feeding in the mesopelagic zone and export of small phytoplankton. Marine Ecology Progress Series 412, 11–27.

Wyman, M., 1992. An in vivo method for the estimation of phycoerythrin concentrations in marine cyanobacteria (*Synechococcus* spp.). Limnology and Oceanography 37, 1300–1306.

Zhang, X., Dam, H.G., White, J.R., Roman, M.R., 1995. Latitudinal variations in mesozooplankton grazing and metabolism in the central tropical Pacific during the US JGOFS EqPac Study. Deep-Sea Research II 42, 695–714.